Palaeogeography, Palaeoclimatology, Palaeoecology 560 (2020) 110018

Contents lists available at ScienceDirect

Palaeogeography, Palaeoclimatology, Palaeoecology

journal homepage: www.elsevier.com/locate/palaeo

A paleoproductivity shift in the northwestern Bay of Bengal (IODP Site U1445) across the Mid-Pleistocene transition in response to weakening of the Indian summer monsoon

Jongmin Lee[a], Sunghan Kim[b,1], Boo-Keun Khim[a,*]

[a] *Department of Oceanography, Pusan National University, Busan 46241, South Korea*
[b] *Division of Polar Paleoenvironment, Korea Polar Research Institute, Incheon 21990, South Korea*

ARTICLE INFO

Keywords:
Organic carbon
Biogenic opal
Calcium carbonate
Organic carbon isotopes
Surface water productivity
Riverine discharge

ABSTRACT

The long-term variability of the Indian monsoon in the Bay of Bengal remains inconclusive due to the lack of proximal sedimentary records. To further elucidate the long-term variability of the Indian monsoon, we analyzed the paleoproductivity regime over the last 2.3 Myr at the International Ocean Discovery Program (IODP) Expedition 353 Site U1445 located near the Mahanadi Basin in the northwestern Bay of Bengal. We measured the downcore concentrations and mass accumulation rates (MARs) of biogenic opal, $CaCO_3$, total organic carbon (TOC), and total nitrogen over the Mid-Pleistocene Transition (MPT) to identify the links between surface water marine biogenic production and the Indian summer monsoon. TOC MARs were found to reflect both surface water marine productivity and terrestrial organic matter through the measurements of sediment C/N ratios and $\delta^{13}C_{SOM}$ values. Nonetheless, we identified a shift in the paleoproductivity regime from a dominance of biogenic opal deposition prior to the MPT to the dominance of $CaCO_3$ deposition following the MPT. The shift in biogenic marine productivity across the MPT was closely related to riverine discharge, which was primarily controlled by the intensity of the Indian monsoon. Our results, therefore, infer a decrease in riverine discharge to the Bay of Bengal across the MPT in response to a weakened Indian summer monsoon (and/or strengthened Indian winter monsoon). In addition, changes in the intensity of the Indian monsoon across the MPT were more closely linked to the global climate cooling rather than the gradual uplift of the Himalaya and Tibetan Plateau.

1. Introduction

The Quaternary Period was characterized by large amplitude and high-frequency climate oscillations (Clark et al. 2006). In particular, the Mid-Pleistocene Transition (MPT: 1.25 to 0.7 Ma) was the most significant interval of global climate change since the advent of Northern Hemisphere glaciation (3.5 to 2.5 Ma) (Maslin et al. 1998). The MPT is generally characterized by a shift in the periodicity of the glacial-interglacial cycles from 41 to 100 kyr (Clark et al. 2006), coinciding with notable changes in high-latitude ice volume (Lisiecki and Raymo 2005), sea level (Rohling et al. 2014), global ocean temperature (Herbert et al. 2010), and monsoonal climate (DeMenocal 1995). In particular, a decline in downcore smectite/(illite + chlorite) ratios in the eastern Arabian Sea (International Ocean Discovery Program (IODP) Site U1456; Fig. 1) inferred a weakening of the Indian summer monsoon following the MPT (Chen et al. 2018).

The strength of the Asian monsoon, which consists of the Indian (or South Asian) and East Asian monsoons, is controlled by global climate variabilities (Gupta et al. 2004) and by the uplift of the Himalayas and Tibetan Plateau (HTP) at the tectonic/orbital time-scale (An et al. 2001), although monsoon changes were affected by various forcing mechanisms (Mohtadi et al. 2016). Global climate influenced degree of wind speed and precipitation amount of Asian summer monsoon between the interglacial (strong wind/high precipitation) and glacial (weak wind/low precipitation) periods (Gebregiorgis et al. 2018; Wang et al. 2019). Climate models have deduced a close relationship between the intensification of the Indian monsoon and the uplift of the HTP (Zhang et al. 2012), as the heat contast during the summer lowers the atmospheric pressure at high altitudes, which in turn strengthens the Indian monsoon (Webster et al. 1998). However, the response of HTP uplift to the Indian monsoon remains still uncertain. Recent studies (Clift et al. 2019; Li et al. 2019) have shown that the strength of the

* Corresponding author.
E-mail address: bkkhim@pusan.ac.kr (B.-K. Khim).
[1] Equally contributed author.

https://doi.org/10.1016/j.palaeo.2020.110018
Received 28 February 2020; Received in revised form 6 September 2020; Accepted 7 September 2020
Available online 10 September 2020

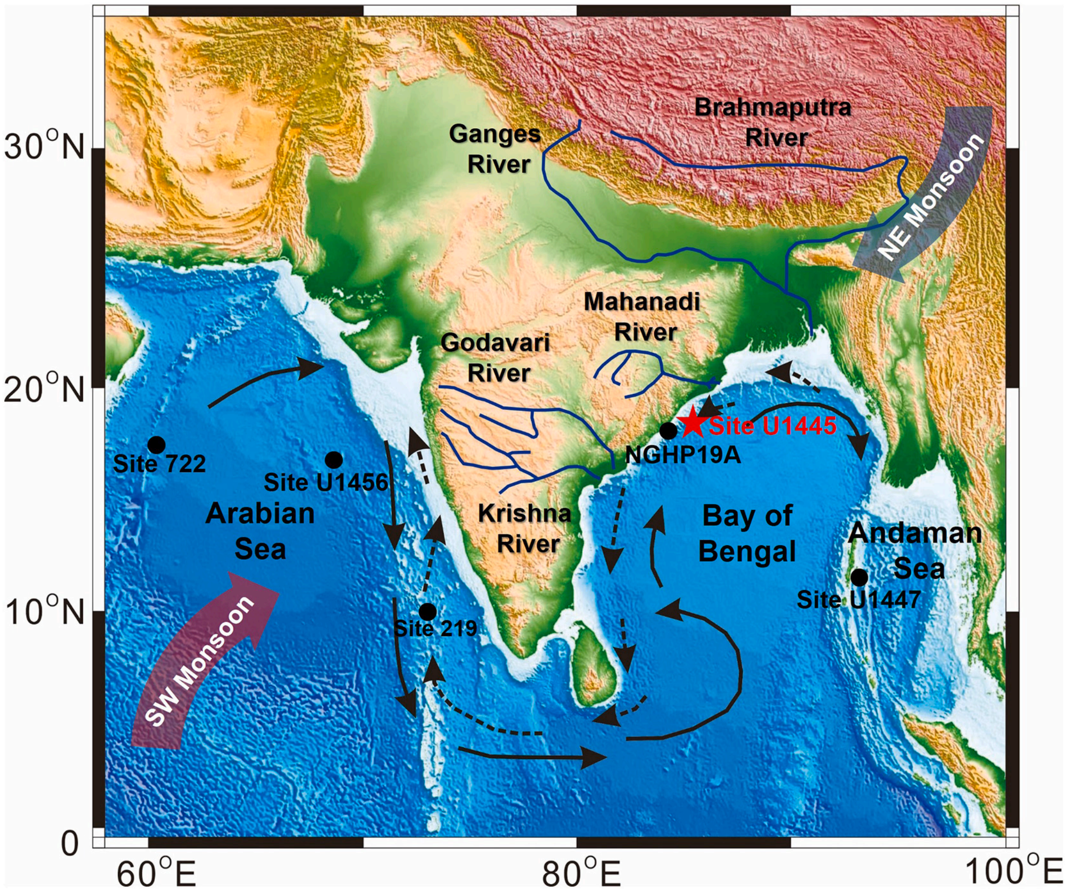

Fig. 1. Location of IODP Site U1445 (red star; this study) in the northwestern Bay of Bengal and other sites (black circles) of previous studies: ODP Site 722 (Huang et al. 2007), IODP Site U1456 (Chen et al. 2018), DSDP Site 219 (Mohan and Gupta 2011), NGHP 19A (Johnson et al. 2014), and IODP Site U1447 (Lee et al. 2020). Solid (summer) and dashed (winter) arrows represent the general surface water currents and red (summer) and blue (winter) arrows mark the direction of the monsoon winds. (For interpretation of the references to colour in this figure legend, the reader is referred to the web version of this article.)

Indian monsoon during the late Miocene to the Pliocene was more closely linked to global climate cooling rather than the HTP evolution.

During the Indian summer monsoon, strengthened southwesterly winds over the Indian Ocean induced by asymmetric heating between the cooler Indian Ocean and the warmer Indo-Asian continent transports large amounts of precipitation to the Peninsula India (Webster and Fasullo 2003). Many studies have, therefore, been conducted in the Bay of Bengal (characterized by the huge submarine fan) to explore the history of Indian summer monsoon and its influence on the marine environment (e.g., Bolton et al. 2013; Phillips et al. 2014; Ota et al. 2018, 2019). Most of these studies focused on orbital time-scales to determine monsoon variability across glacial-interglacial cycles. However, only a small number of studies in the equatorial Indian Ocean or the southern Bay of Bengal have investigated the monsoon variability on tectonic time-scales (e.g., Gupta et al. 2004; Banerjee et al. 2019). These distal records were unable to adequately capture major and subtle changes in monsoonal rainfall, such as the potential decrease in sea surface salinity in the northern Bay of Bengal in response to the Indian summer monsoon.

The Bay of Bengal receives high riverine discharge from the Ganges-Brahmaputra, Mahanadi, Krishna, and Godavari rivers, particularly during the Indian summer monsoon (Fig. 1). Large riverine discharge and strong stratification during the monsoon season were found to reduce coastal upwelling in the Bay of Bengal, which supplies subsurface nutrients to the surface water (Ramaswamy and Gaye 2006). However, due to the complex oceanographic/hydrographic processes in the region, the influence of the Indian summer monsoon on surface water productivity in the northern Bay of Bengal is still ambiguous. For examples, some studies have reported reduced surface water productivity due to strong stratification, cloud cover, and increased turbidity (e.g., Madhupratap et al. 2003). In contrast, other studies have reported enhanced surface water productivity due to increased nutrient supply by riverine input or by eddy pumping (e.g., Prasanna Kumar et al. 2004). It is, therefore, necessary to improve our understanding of the relationship between surface water productivity and the Indian summer monsoon in the northern Bay of Bengal.

In this study, we present a multi-proxy sediment record (total nitrogen [TN], total organic carbon [TOC], biogenic opal, $CaCO_3$, and $\delta^{13}C$ of sediment organic matter [$\delta^{13}C_{SOM}$]) representing surface water marine productivity at IODP Site U1445 in the northwestern Bay of Bengal over the last 2.3 Myr (Fig. 1). Our results shed light on the relationship between surface water productivity and the Indian summer monsoon, particularly across the prominent global climate shift of the MPT.

2. IODP Site U1445 in the northwestern Bay of Bengal

The Bay of Bengal comprises the largest submarine fan in the world, which covers an area of ~3 × 10^6 km^2 and reaching a water depth of ~5000 m (Curray et al. 2002). The bay is a semi-enclosed tropical basin in the northern Indian Ocean and is surrounded by the Peninsula India to the west, Bangladesh to the north, and Myanmar and the Andaman and Nicobar Islands to the east (Fig. 1). Seasonal monsoon climate in the Bay of Bengal controls surface water circulation: cyclonic (southwesterly wind) surface current dominates in summer and anti-cyclonic (northeasterly wind) surface current dominates in winter (Fig. 1; Schott and McCreary Jr, 2001). More than 90% of the total annual freshwater (10 × 10^{12} m^3) and terrigenous sediment (15 × 10^6 metric tons) discharge to the bay occurs during the summer season (Chakrapani and Subramanian 1990).

Elevated freshwater input during the summer monsoon increases water column stratification in the northern Bay of Bengal (Narvekar and Kumar 2014). Stratifiation reduces upwelling and subsequently limits the upward supply of nutrients. For example, low (< 1 μM) nitrate concentrations were observed off the coast of the northern Bay of Bengal in the upper 50 m of the water column during late summer and post-monsoon period (Madhupratap et al. 2003). Primary productivity in the surface water, therefore, decreased toward the open ocean where diatoms dominate the phytoplankton assemblage.

IODP Expedition 353 drilled at seven sites in the Bay of Bengal and the Andaman Sea from Nov. 2014 to Jan. 2015 (Clemens et al., 2016). IODP Site U1445 (17°44.72′N, 84°47.25′E; 2513 m water depth) consists of three drilled holes (Holes U1445A, U1445B, and U1445C) in a flat-lying upper continental rise located near the southern end of the Mahanadi Basin in the northwestern Bay of Bengal (Fig. 1). Lithologic units at IODP Site U1445 were determined onboard by visual core descriptions, smear slide examinations, physical property, and X-ray diffraction data (Clemens et al., 2016). Only one lithostratigraphic unit was reported at this site due to the homogenous nature of the sediments, which were further subdivided into two subunits (Subunits Ia: 0–165.28 m CSF-A and Ib: 165.28–667.56 m CSF-A) based on the nannofossil and biosilica contents determined from preliminary microscopic examination (Fig. 2). Sediments were mostly composed of hemipelagic clays with a large biogenic component and the occasional thin turbidite.

A preliminary chronostratigraphic framework at IODP Site U1445 was also established onboard based on magnetostratigraphy and biostratigraphic data of calcareous nannofossils, planktonic foraminifera, and diatoms (Clemens et al., 2016). In brief, the occurrence of the oldest calcareous nannofossil (*Discoaster quinqueramus*) at Hole U1445A infers an age of 5.59 Ma, and the occurrence of planktonic foraminifera (*Globigerinoides conglobatus*) marks a maximum age of 6.20 Ma. The last occurrence of the oldest diatom *Nitzschia miocenica* records an age of 5.7 Ma. Combined biostratigraphic data indicate a core age of ~6 Ma (late Miocene) at IODP Site U1445 (Fig. 2).

3. Materials and methods

We collected a total of 175 downcore sediment samples at discrete (~1.37 m) intervals from 4 to 242 m CSF-A at Hole U1445A (17°44.72′N, 84°47.25′E; 2513 m water depth). The samples cover the last 2.3 Myr (Fig. 2), and the age of each sample was determined using linear interpolation based on previously determined age data reported in Clemens et al. (2016).

TC and TN contents of each sample were measured using a Flash 2000 Series Elemental Analyzer at Pusan National University with an analytical precision of less than ± 0.1% and ± 0.01%, respectively. Total inorganic carbon (TIC) concentrations were also measured using a UIC CO_2 Coulometer (Model CM5240) at Korea Polar Research Institute (KOPRI), and $CaCO_3$ concentrations were calculated by multiplying TIC concentration by 8.333 (the molecular weight ratio between $CaCO_3$ and C). TOC concentrations were calculated as the difference between TC and TIC contents. C/N ratios were calculated as the ratio of TOC to TN contents. To measure biogenic silica (Si_{Bio}) content, we followed a wet alkaline extraction method modified from DeMaster (1981) using a Continuous Flow Analyzer (SKALAR SAN^{plus} Analyzer) at KOPRI, with a relative error of less than ± 1%. The biogenic opal content was calculated by multiplying Si_{Bio} content by 2.4 (Mortlock and Froelich 1989). Following 10% HCl treatment for $CaCO_3$ removal, we measured $\delta^{13}C_{SOM}$ values of 54 selected samples by elemental analysis-isotope ratio mass spectrometry (EA-IRMS: Europa Scientific 20–20 mass spectrometer) at Iso-Analytical Ltd. (UK). The analytical precision for $\delta^{13}C_{SOM}$ was approximately ± 0.08‰.

Mass accumulation rate (MAR) for TN, TOC, biogenic opal, and $CaCO_3$ was calculated as follows: Biogenic component (TN, TOC, biogenic opal, and $CaCO_3$) MAR (g/cm^2/kyr) = biogenic component content × DBD (dry bulk density) (g/cm^3) × LSR (linear sedimentation rate) (cm/kyr). The DBD was measured onboard from discrete samples at approximately 3 m intervals (Clemens et al., 2016). The LSR was calculated based on the slope of the age-depth plot at each interval.

4. Results

We identified three intervals based on the downcore variability of geochemical properties (TN, TOC, biogenic opal, and $CaCO_3$) at IODP Site U1445: pre-MPT (2.3–1.5 Ma), the MPT (1.5–0.8 Ma), and post-MPT (0.8–0 Ma) (Fig. 3a to h). The pre-MPT interval was characterized by high TN (av. 0.16%), TOC (av. 1.69%), and biogenic opal (av. 7.4%) contents, and low $CaCO_3$ (av. 2.9%) content. TN (0.19% to 0.07%, av. 0.13%), TOC (2.1% to 0.8%, av. 1.4%), and biogenic opal (11.1% to 1.5%, av. 4.4%) contents gradually decreased and the $CaCO_3$ content

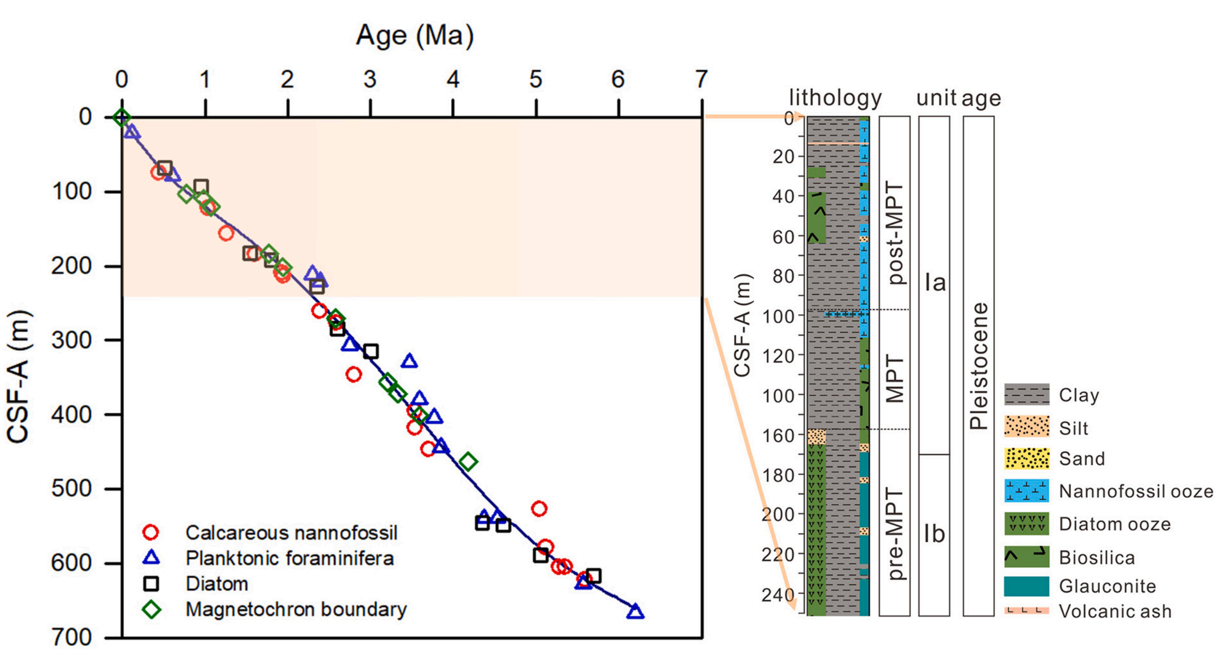

Fig. 2. The age model and lithology for IODP Site U1445 (Clemens et al., 2016).

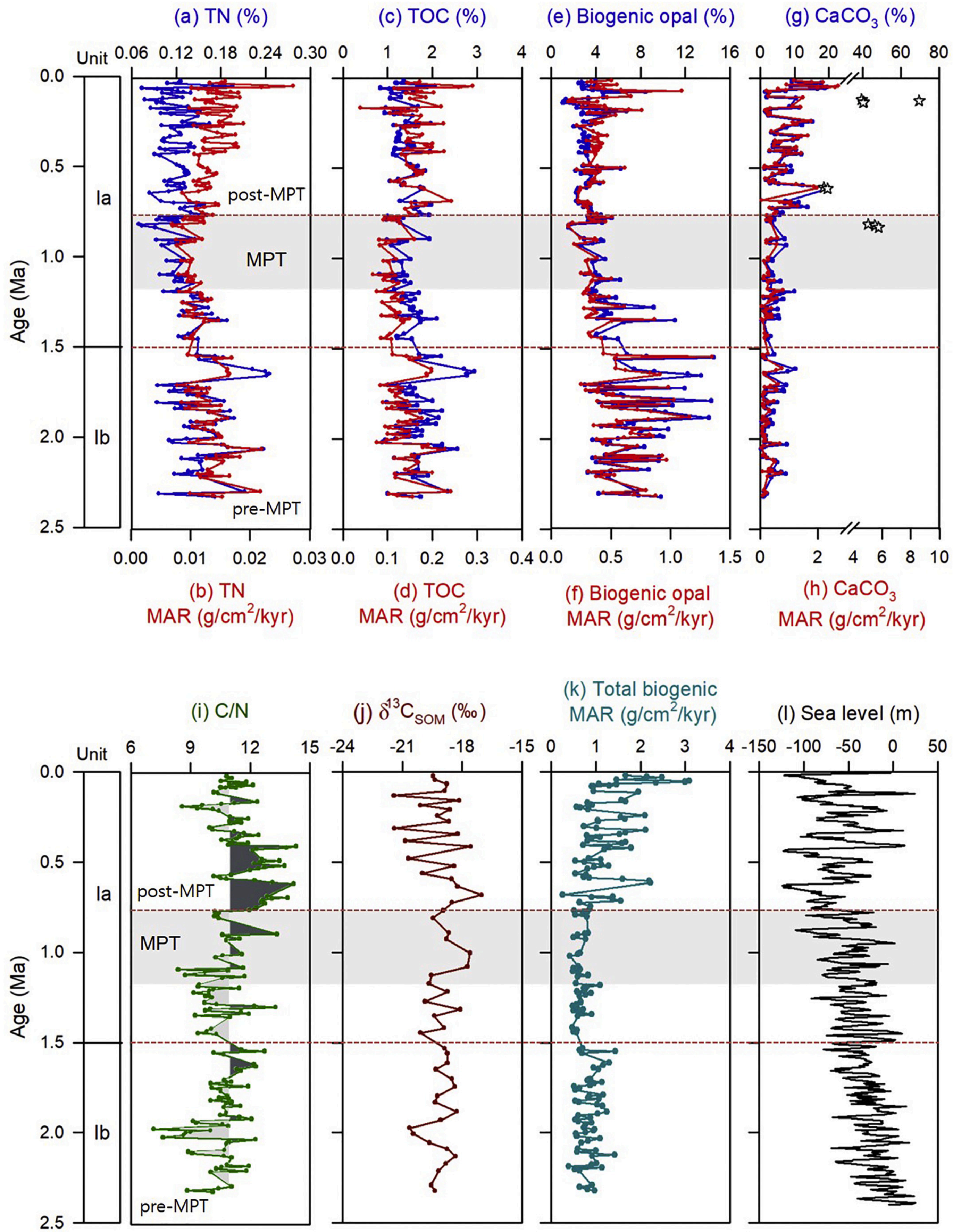

(caption on next page)

Fig. 3. Downcore variations of geochemical properties at IODP Site U1445 alongside the global sea level record (Miller et al. 2005) over the last 2.3 Myr: (a) TN content, (b) TN MAR, (c) TOC content, (d) TOC MAR, (e) biogenic opal content, (f) biogenic opal MAR, (g) $CaCO_3$ content, (h) $CaCO_3$ MAR, (i) C/N ratio, (j) $\delta^{13}C_{SOM}$ value. White stars represent authigenic carbonates (Clemens et al., 2016). The shaded interval marks the Mid-Pleistocene Transition (MPT).

increased (0.6% to 10.0%, av. 3.7%) during the MPT interval. The post-MPT interval showed opposite geochemical trends to the pre-MPT interval and was characterized by low TN (av. 0.12%), TOC (av. 1.4%) and biogenic opal (av. 3.4%) contents, and high $CaCO_3$ (av. 7.6%) contents. We observed intermittent peaks in $CaCO_3$ content (> ~20%) due to abundant authigenic carbonate (Clemens et al., 2016). The MARs of biogenic opal and $CaCO_3$ were in good agreement with their contents (Fig. 3b and h), but TN and TOC MARs increased slightly in the post-MPT interval (Fig. 3b and d). Compared with the post-MPT interval, the frequent fluctuations of biogenic opal content and MARs (Fig. 3e and f) with TN and TOC records were recognizable in the pre-MPT interval. More frequent fluctuation of $CaCO_3$ content and MARs occurred during the post-MPT interval (Fig. 3g and h).

C/N ratios at IODP Site U1445 ranged from 7 to 14 over the last 2.3 Myr, showing a slight increase from pre-MPT (7 to 13, av. 11) to post-MPT (9 to 14, av. 12) interval across the MPT (8 to 13, av. 11) interval (Fig. 3i). Downcore $\delta^{13}C_{SOM}$ values generally showed minor variability, ranging from −21‰ to −17‰ (av. -19‰); the post-MPT interval was characterized by large $\delta^{13}C_{SOM}$ fluctuations (Fig. 3j).

5. Discussion

5.1. Paleoproductivity variability at IODP Site U1445 since 2.3 Ma

TOC and TN contents of marine sediments are indicative of organic matter accumulation and can be related to surface water primary productivity, preservation potential, and/or terrestrial organic input (Stein 1991). The strong positive correlation (r^2 = 0.71 to 0.87; Fig. 4a) between TOC and TN contents at IODP Site U1445 confirms common source of TOC and TN during the last 2.3 Myr, despite the positive intercept of each regression line represents the incorporation of inorganic nitrogen to a certain extent. During the pre-MPT, TOC contents are strongly correlated with the biogenic opal contents, compared with $CaCO_3$ contents (Fig. 4b and c). These results suggest that the higher TOC and TN contents during the pre-MPT interval may be attributed to increased biogenic opal production (i.e. marine productivity) rather than contributions of terrestrial organic matter. Given that C/N ratios of marine organic matter (phytoplankton; 5–10) are lower than those of terrestrial vascular plants (> 12) (Meyers 1994), the range of C/N ratios at IODP Site U1445 (7 to 15, av. 11) imply a mixture of marine and terrestrial organic matters in sediments (Fig. 3i). Sediment C/N ratios increased during the post-MPT interval. Nonetheless, it is difficult to estimate terrestrial organic matter incorporation at this site due to the statistically poor correlation coefficients (Fig. 4d). Similarly, the $\delta^{13}C_{SOM}$ values at IODP Site U1445 also confirm a mixture of marine and terrestrial organic matters in the sediments (Fig. 4e) and the lower $\delta^{13}C_{SOM}$ values occurred during the post-MPT interval (Fig. 3j). These simultaneous changes of higher C/N ratios and lower $\delta^{13}C_{SOM}$ values at IODP Site U1445 may be attributed to a relatively increased contribution of terrigenous organic matter while the global mean sea level was low during the post-MPT interval (Fig. 3l; Miller et al. 2005). Thus, it seems that the contribution of organic matters at IODP Site U1445 has been changed from marine production to terrestrial organic matters over the last 2.3 Myr, despite the mixture of marine and terrestrial organic matters.

Diatoms account for > 90% of the total phytoplankton bloom in the present-day Bay of Bengal (Madhupratap et al. 2003) and thus play an important role in transporting organic carbon to the deep seafloor (Ramaswamy and Gaye 2006). Moreover, Ragueneau et al. (2000) suggested that the preservation efficiency of biogenic opal is closely related to the in situ sedimentation rate. As such, the fairly high sedimentation rate (~12 cm/kyr; Clemens et al., 2016) at IODP Site U1445 facilitates the preservation of biogenic opal in the deep seafloor. It is difficult to assess the dissolution effect of biogenic silica within the water column in the Bay of Bengal; however, it is assumed to be fairly constant between 1000 and 3000 m water depth (Nelson et al. 1995). Thus, we conclude that the biogenic opal MARs at IODP Site U1445 are an adequate proxy for biogenic siliceous production in the surface waters of the Bay of Bengal.

The relative concentrations of macronutrients – such as silicate, nitrate, and phosphate – have been shown to mainly influence the phytoplankton community structure in the Bay of Bengal (Paul et al. 2008), although there are the other important controlling factors such as temperature, pCO_2, and trace metals (Boyd et al. 2010; Smith et al. 2017). Silicate, in particular, plays an important role in determining diatom growth rates (Officer and Ryther 1980). The Ganges-Brahmaputra rivers and the river systems of the Peninsular India supply large amounts of dissolved silicate to the Bay of Bengal (Prasanna Kumar et al. 2002). Diatom biomass tends to decrease with distance from the river mouth where silicate concentrations are highest (> 4 μM) (Madhupratap et al. 2003). Sarma et al. (2016) also observed higher silicate concentrations relative to nitrate and phosphate in the low saline waters of the northern Bay of Bengal, suggesting that the freshwater is a main source of silicate to the Bay of Bengal. Moreover, in the northwestern Bay of Bengal, maximum and minimum silicate concentrations were observed in July (monsoon season) and March (pre-monsoon season), respectively (Miranda et al. 2019). Consequently, siliceous phytoplankton production (i.e., diatom) in the Bay of Bengal predominantly depends on the degree of riverine discharge, with high diatom production under increased runoff.

According to previous shipboard data (Clemens et al., 2016), the main $CaCO_3$ components at IODP Site U1445 are nannofossils and foraminiferas. In this study, the authigenic carbonate content (> 20%) was not considered for carbonate production (Fig. 3g and h; white stars). The temporal variations in $CaCO_3$ MARs in the Bay of Bengal were mainly controlled by the calcite production (Naidu and Malmgren, 1999) and differential preservation (George et al. 1994). The calcite saturation depth or lysocline in the Bay of Bengal is ~3000 m (Sabine et al. 2002), which is deeper than the water depth (~2500 m) at IODP Site U1445. The $CaCO_3$ particle fluxes of sediment traps between the shallow (730–810 m) and deep (1730–2300 m) water in the northern Bay of Bengal were not distinctly different (Unger et al. 2003). Moreover, Clemens et al. (2016) reported that the preservation of calcareous nannofossils and foraminiferas was moderate to good throughout the most studied interval at IODP Site U1445. On the other hand, it was also reported that the carbonate preservation (i.e., dissolution) was affected by the variations of aragonite compensation depth (ACD) during the late Quaternary in the northern Indian Ocean such as the Andaman Sea and Arabian Sea (Reichart et al. 1998; Sijinkumar et al. 2010). The sedimentation rate was used to calculate $CaCO_3$ MARs, which accounts for the dilution effect of lithogenic material. The calculated $CaCO_3$ MARs at IODP Site U1445 are therefore independent of the terrigenous sediment dilution effect, and thus the production and preservation of calcareous marine organisms might be the major factors contributing to the $CaCO_3$ MARs changes.

Nitrogen influx was found to significantly influence calcareous production in the Indian Ocean (Prasanna Kumar et al. 2007). Prasanna Kumar et al. (2002) reported that freshwater runoff was not a significant source of nitrate to the Bay of Bengal. In the northern Bay of Bengal, stratification caused by increased river discharge weakens upwelling and limits nitrate supply into the euphotic zone (Prasanna Kumar et al. 2002; Madhupratap et al. 2003). Coastal upwelling is, therefore, the principal control on the biogenic calcareous production in the northwestern Bay of Bengal due to insufficient riverine supply of nitrate relative to silicate (Sarma et al. 2016). As described previously, upwelling in the northern Bay of Bengal is suppressed by higher riverine freshwater discharge. In agreement, the highest nitrate concentrations in the northern Bay of Bengal were observed in the low riverine discharge season under increased coastal upwelling. For

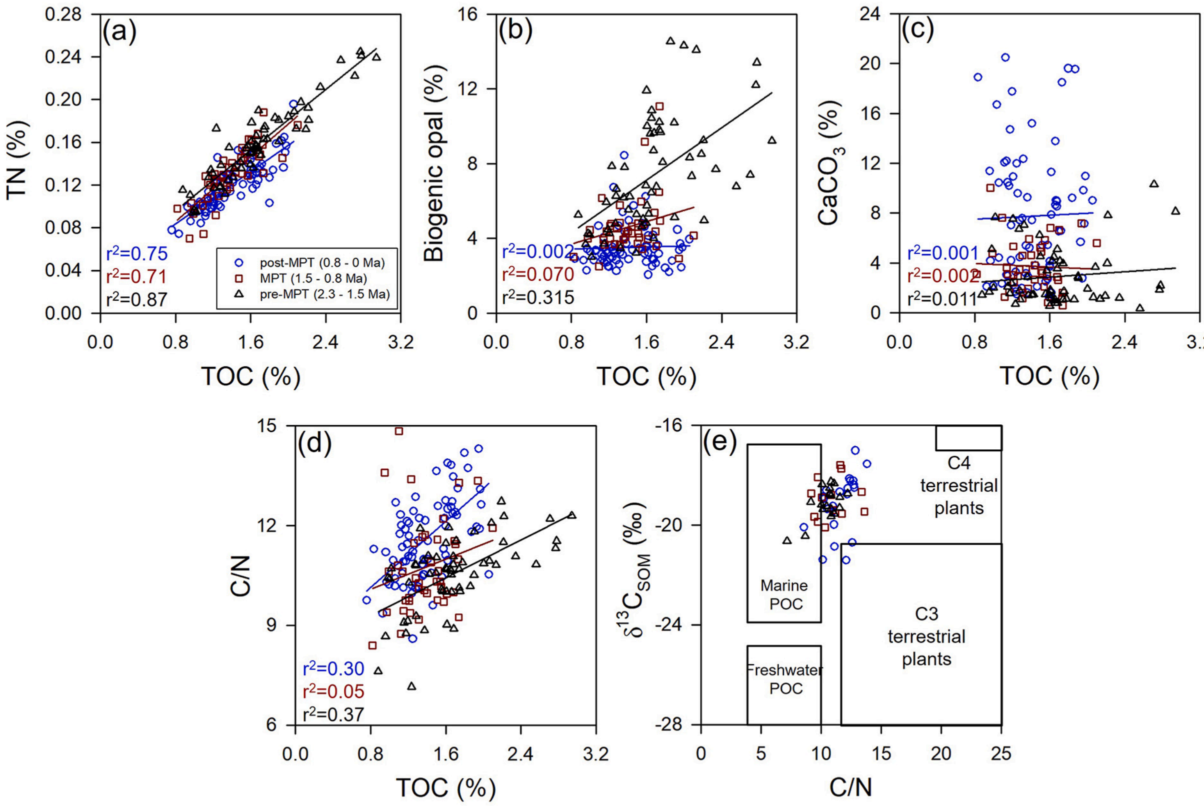

Fig. 4. (a) Correlation between TOC and TN contents, (b) Correlation between TOC and Biogenic opal contents, (c) Correlation between TOC and $CaCO_3$ contents, (d) Correlation between TOC and C/N ratios, and (e) Correlation between C/N ratios and $\delta^{13}C_{SOM}$ values at IODP Site U1445 over the last 2.3 Myr.

example, the maximum of nitrate concentrations was observed in the northwestern Bay of Bengal in October (weak precipitation season), while the minimum of its occurred in July (strong precipitation season) (Miranda et al. 2019). Hence, the $CaCO_3$ MARs at IODP Site U1445 may reflect riverine freshwater influx and upwelling activity with higher biogenic calcareous production under lower riverine discharge.

According to the previous studies (Reichart et al., 1998; Sijinkumar et al. 2010), carbonate preservation related to the dissolution can be also a significant factor to control the variations of $CaCO_3$ MARs in marine sediments because the northern Indian Ocean is characterized by the deepening of ACD during the winter monsoon (weak precipitation season). Sijinkumar et al. (2010) observed that the pteropod abundance and its preservation pattern were better during the glacial periods than the interglacial periods in the Andaman Sea due to the deeper ACD. Similarly, the deepening of ACD during the glacial periods also occurred in the Arabian Sea (Reichart et al. 1998). These results suggested that ACD was considerably deeper during the glacial periods in the Bay of Bengal, which resulted in the better preservation of calcareous matters. During the post-MPT, the $CaCO_3$ contents and MARs increased significantly at IODP Site U1445 during the sea level low stand intervals (i.e. cold periods) (Fig. 3). Therefore, we concluded that the decreased freshwater caused the enhanced biogenic calcareous production and the deepening of ACD induced less dissolution of biogenic carbonate at IODP Site U1445 during the cold periods.

In summary, our results demonstrate that downcore biogenic opal and $CaCO_3$ MARs at IODP Site U1445 reflect the biological production of marine siliceous and calcareous organisms in the surface water of the northwestern Bay of Bengal over the last 2.3 Myr. Furthermore, their variations are closely related to riverine discharge, with high biogenic opal and low $CaCO_3$ MARs under high riverine discharge and vice versa. Our results are consistent with the suggestion of Phillips et al. (2014), emphasizing a critical role of river discharge and upwelling in surface water productivity in the northwestern Bay of Bengal, despite different time slice.

5.2. Influence of Indian monsoon on paleoproductivity across the MPT

Over the last 2.3 Myr, MARs and concentrations of biogenic opal fairly showed opposite trends to those of $CaCO_3$ at IODP Site U1445. Although the frequent fluctuations of biogenic opal MARs were recognizable in the pre-MPT, it is difficult to be explained clearly because the current age model is not as high-resolution as the orbital timescale. Nonetheless, we observed a shift from a dominance of biogenic opal during the pre-MPT to the dominance of biogenic $CaCO_3$ during the post-MPT across the MPT (Fig. 3f and h). This long-term change in paleoproductivity imply a gradual decrease in freshwater discharge to the northwestern Bay of Bengal from the pre-MPT to the post-MPT. This result is supported by the observed increase in total (biogenic opal + $CaCO_3$) biogenic MARs since the MPT (Fig. 3k). Marine biogenic production was not uniformly represented by biogenic opal or $CaCO_3$ MARs; therefore, their sum more accurately represents total biogenic production, despite the exclusion of non-siliceous and non-calcareous organisms (e.g., cyanobacteria and dinoflagellates) (Phillips et al. 2014). Low total biogenic production was observed under high riverine discharge during relatively warm periods in the northern Bay of Bengal (Phillips et al. 2014; Ota et al. 2019). Our study also confirms lower total biogenic MARs at IODP Site U1445 under the relatively warmer climate of the pre-MPT interval relative to the cooler climate of the post-MPT interval.

The multi-proxy dataset of long-term climate variability is shown in Fig. 5, signifying a weakening of the Indian summer monsoon (or a strengthening of the Indian winter monsoon) since 2.3 Ma. The paleoproductivity regime shift over the MPT in response to the gradual decrease in riverine discharge (Fig. 5b) coincided with long-term global climate cooling (Fig. 5a). Clemens et al. (2016) reported an increase in the proportion of clay-sized particles at IODP Site U1445 from the pre-MPT to the post-MPT (Fig. 5c). Cao et al. (2015) also observed higher deposition rates of clay-sized particles under low precipitation and riverine discharge in the Andaman Sea. Moreover, lower sea levels

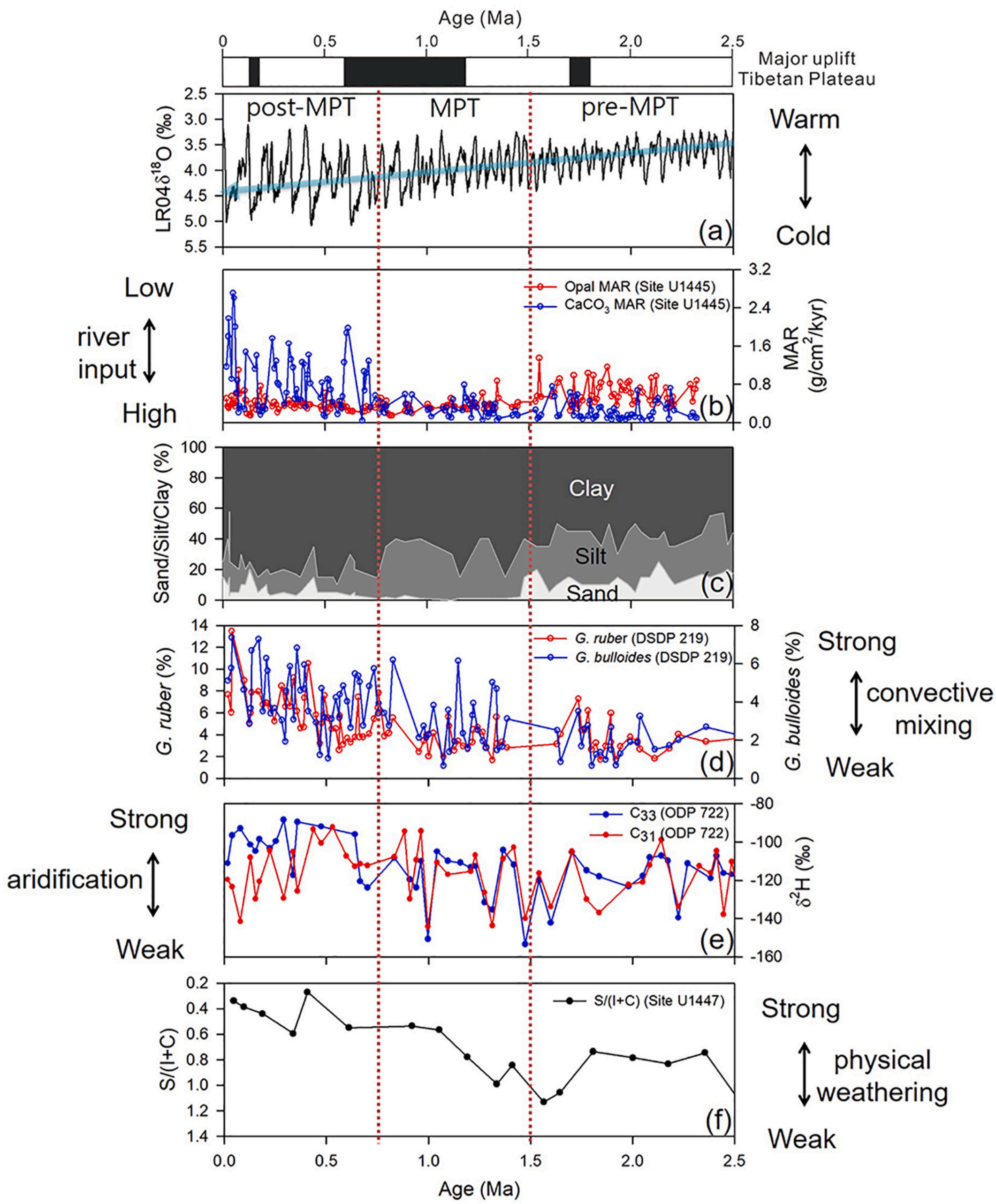

Fig. 5. Comparisons of (a) major uplift events (black bars) of the HTP over the last 2.5 Myr (Li et al. 2014) with global climate variability inferred from deep-sea benthic foraminiferal oxygen isotopes (Lisiecki and Raymo 2005), (b) biogenic opal and $CaCO_3$ MARs at IODP Site 1445 (this study), (c) the sand-silt-clay composition at IODP Site U1445 (Clemens et al., 2016), (d) planktonic foraminiferal abundance (*Globigerina bulloides* and *Globigerinoides ruber*) at DSDP Site 219 (Mohan and Gupta 2011), (d) the δ^2H of n-C_{31} and n-C_{33} alkanes at ODP Site 722 (Huang et al. 2007), and (e) smectite/(illite + chlorite) ratios at IODP Site U1447 (Lee et al. 2020).

facilitated the delivery of terrigenous organic matter to the deeper basin following the MPT (Rohling et al. 2014). Mohan and Gupta (2011) reported an increase in mixed-layer planktonic foraminiferal species (i.e., *Globigerinoides ruber* and *Globigerina bulloides*) from the pre-MPT to the post-MPT at Deep Sea Drilling Project Site 219 in the southeastern Arabian Sea (Fig. 5d); this was attributed to intense deep convection caused by a strengthening of the Indian winter monsoon since 3.4 Ma. Lower δ^2H values of long-chain n-alkanes in sediments at Ocean Drilling Program (ODP) Site 722 in the western Arabian Sea since the late Miocene (Fig. 5e) suggested increased aridification in the Indus River basin in response to a weakening of the Indian summer monsoon (Huang et al. 2007). Decreasing S/(I + C) ratios at IODP Site U1447 (Fig. 5f) reflected intensified physical weathering from the pre-MPT to the post-MPT in the Andaman Sea in response to a weakening (strengthening) of the Indian summer (winter) monsoon in the Myanmar region (Lee et al. 2020). Collectively, these results imply a weakening of the Indian summer monsoon from the pre-MPT to post-MPT across the MPT.

In general, the amount of riverine discharge depends on the intensity of monsoonal precipitation, with higher precipitation occurring during the warmer interglacial (Govil and Naidu, 2011). The intensity of riverine discharge was shown to influence marine plankton assemblages over the past 80 kyr in the northwestern Bay of Bengal, with enhanced biogenic siliceous (calcareous) production under higher (lower) riverine discharge of interglacial (glacial) periods (Ota et al. 2019). In agreement, we revealed high biogenic opal MARs during the warmer pre-MPT and high $CaCO_3$ MARs during the cooler post-MPT interval. Considering an important role of river discharge and

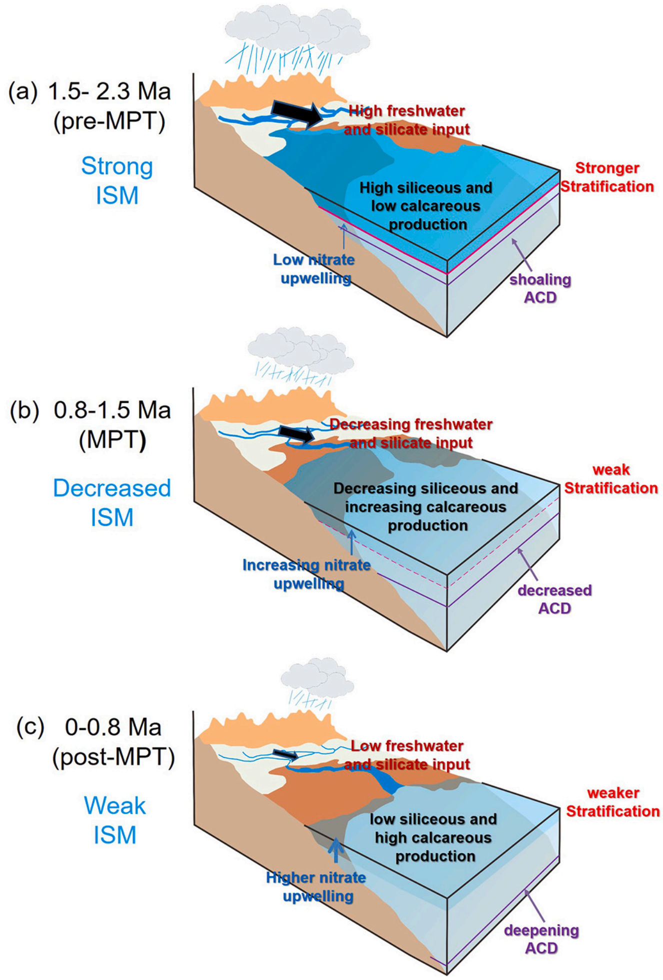

Fig. 6. Schematic illustration of the paleoceanographic change with the paleoproductivity condition in the northwestern Bay of Bengal since 2.3 Ma (modified from Phillips et al. 2014), including (a) the pre-MPT interval, (b) the MPT, (c) the post-MPT interval.

upwelling in surface water productivity (Phillips et al. 2014), Fig. 6 depicts the schematic paleoceanographic setting of the northwestern Bay of Bengal in response to monsoonal evolution over the last 2.3 Myr. During the pre-MPT, high riverine discharge under strong Indian summer monsoonal precipitation enhanced the supply of silica and subsequently increased biogenic siliceous production (i.e., diatoms) in the northwestern Bay of Bengal, while strong stratification led to a decrease in calcareous production by preventing the supply of nitrate to the surface water. The shoaling ACD also influenced low preservation of calcareous matters (Fig. 6a). The flux of riverine freshwater gradually decreased across the MPT in response to a weakening of Indian summer monsoon, resulting in reduced silica supply for biogenic siliceous production and weaker stratification led to simultaneously a slight increase in biogenic calcareous production, which increased the supply of nitrate to the surface water. Lowering ACD helps preservation of calcareous matters (Fig. 6b). A further weakening of the Indian summer monsoon during the post-MPT reduced freshwater discharge, which resulted in the biogenic siliceous production due to the lowered riverine silica supply. On the other hand, weakened stratification stimulated calcareous production by promoting the upwelling of nitrate to the surface waters. In addition, the deepening of ACD resulted in better preservation of calcareous matters (Fig. 6c).

Two controlling mechanisms on the past variability of the Asian monsoon (including the Indian and East Asian monsoons) at tectonic/orbital time-scale have been proposed: 1) the HTP uplift (An et al. 2001) and 2) global climate variability (Gupta et al. 2004; Lu et al. 2010). The Indian summer monsoon intensified during the 'phased uplift of the HTP' (An et al. 2001; Tang et al. 2013). Li et al. (2014) reported that the HTP experienced a series of significant uplift events (i.e., ~8, ~3.6, ~2.6, 1.8–1.7, 1.2–0.6, and 0.15 Ma) since the late Miocene (Fig. 5a). For example, the observed shift in the clay mineral assemblage at ~7 Ma from illite-chlorite to smectite-kaolinite in ODP Leg 116 at the Bengal Fan signified a shift to a warmer and more humid climate that facilitated chemical weathering (France-Lanord et al. 1993). In addition, Cai et al. (2018) reported a shift in the terrigenous sediment composition at 3.2 and 1.2 Ma at IODP Site U1456 in the eastern Arabian Sea attributed to the HTP uplift. It is therefore likely that the HTP uplift significantly influenced the past intensity of the Indian monsoon. However, we found that long-term global climate cooling exerted higher control on the gradual weakening of the Indian summer monsoon since 2.3 Ma, despite uplift of the HTP throughout the Quaternary period (Li et al. 2014). Our results suggest that global climate cooling across the MPT was the dominant control on the evolution of the Indian summer monsoon, as indicated by the shift in paleoproductivity regime in the northwestern Bay of Bengal over the last 2.3 Myr.

6. Conclusions

The Indian summer monsoon significantly influences freshwater discharge to the Bay of Bengal from the Ganges-Brahmaputra rivers and other river systems from the Peninsula India. In this study, we analyzed the downcore sedimentary records of paleoproductivity proxies (TN, TOC, biogenic opal, $CaCO_3$, and $\delta^{13}C_{SOM}$) at IODP Site U1445 in the northwestern Bay of Bengal to determine the relationship between marine productivity and the Indian monsoon across the MPT. TOC MARs represented a mixture of terrestrial organic matter and marine biogenic sources based on the C/N ratio and $\delta^{13}C_{SOM}$ records. However, the contribution of organic matters has been changed from marine production to terrestrial organic matters since 2.3 Ma. While, biogenic opal and $CaCO_3$ MARs can reflect surface water marine productivity over the last 2.3 Myr. In particular, we identified a clear shift from the dominance of biogenic opal deposition prior to the MPT to the dominance of $CaCO_3$ deposition following the MPT. High silicate supply to the Bay of Bengal in response to elevated freshwater discharge led to enhanced diatom production at the pre-MPT. In contrast, reduced freshwater discharge following the MPT elevated the nitrate supply from increased upwelling, which promoted $CaCO_3$ production. Moreover, the deepening of ACD resulted in the better preservation of calcareous matters during the post-MPT. The notable shift in the paleoproductivity regime across the MPT was likely linked to the change in riverine discharge governed by the intensity of the Indian monsoon. In addition, we found that the long-term variability of the Indian monsoon across the MPT coincided with global climate cooling rather than the uplift of the HTP. The sampling resolution of our study is too low to capture glacial-interglacial variability (41 to 100 kyr across the MPT); however, our findings significantly contribute to the understanding of the long-term variability of the Indian monsoon based on paleoproductivity changes in the northwestern Bay of Bengal over the last 2.3 Myr.

Declaration of Competing Interest

The authors declare that they have no known competing financial interests or personal relationships that could have appeared to influence the work reported in this paper.

Acknowledgements

We would like to thank crew and all shipboard scientists of IODP Expedition 353. We also thank everyone in the core sampling parties for their assistance in core sampling which took place during November-December 2009 and March 2010 at Kochi Core Center, Kochi

University/JAMSTEC. Thanks also go to Prof. Anil K. Gupta (Indian Institute of Technology Kharagpur) and Prof. K. Mohan (Vellore Institute of Technology) for providing the planktonic foraminifera data. Finally, the manuscript has benefitted from the thoughtful and thorough reviews of editor and two anonymous reviewers. This research was supported by the National Research Foundation of Korea (2016R1A2B4008256 and 2019R1A2C1007701 to BKK) and partly KOPRI (PE20180 to SK).

Appendix A. Supplementary data

Supplementary data to this article can be found online at https://doi.org/10.1016/j.palaeo.2020.110018.

References

An, Z., Kutzbach, J.E., Prell, W.L., Porter, S.C., 2001. Evolution of Asian monsoons and phased uplift of the Himalaya–Tibetan plateau since late Miocene times. Nature 41, 62–66. https://doi.org/10.1038/35075035.

Banerjee, B., Ahmad, S.M., Babu, E., Padmakumari, V., Beja, S.K., Satyanarayanan, M., Krishna, A.K., 2019. Geochemistry and isotopic study of southern Bay of Bengal sediments: implications for provenance and paleoenvironment during the middle Miocene. Palaeogeogr. Palaeoclimatol. Palaeoecol. 514, 156–167. https://doi.org/10.1016/j.palaeo.2018.10.022.

Bolton, C.T., Chang, L., Clemens, S.C., Kodama, K., Ikehara, M., Medina-Elizalde, M., Paterson, G.A., Roberts, A.P., Rohling, E.J., Yamamoto, Y., 2013. A 500,000 year record of Indian summer monsoon dynamics recorded by eastern equatorial Indian Ocean upper water-column structure. Quat. Sci. Rev. 77, 167–180. https://doi.org/10.1016/j.quascirev.2013.07.031.

Boyd, P.W., Strzepek, R., Fu, F., Hutchins, D.A., 2010. Environmental control of open-ocean phytoplankton groups: now and in the future. Limnol. Oceanogr. 55, 1353–1376. https://doi.org/10.4319/lo.2010.55.3.1353.

Cai, M., Xu, Z., Clift, P.D., Khim, B.-K., Lim, D., Yu, Z., Kulhanek, D.K., Li, T., 2018. Long-term history of sediment inputs to the eastern Arabian Sea and its implications for the evolution of the Indian summer monsoon since 3.7 Ma. Geol. Mag. 1–12. https://doi.org/10.1017/S0016756818000857.

Cao, P., Shi, X., Li, W., Liu, S., Yao, Z., Hu, L., Khokiattiwong, S., Kornkanitnan, N., 2015. Sedimentary responses to the Indian Summer Monsoon variations recorded in the southeastern Andaman Sea slope since 26 ka. J. Asian Earth Sci. 114, 512–525. https://doi.org/10.1016/j.jseaes.2015.06.028.

Chakrapani, G., Subramanian, V., 1990. Factors controlling sediment discharge in the Mahanadi River Basin, India. J. Hydrol. 117, 169–185.

Chen, H., Xu, Z., Clift, P.D., Lim, D., Khim, B.-K., Yu, Z., 2018. Orbital-scale evolution of the Indian summer monsoon since 1.2 Ma: evidence from clay mineral records at IODP Expedition 355 Site U1456 in the eastern Arabian Sea. J. Asian Earth Sci. 174, 11–22. https://doi.org/10.1016/j.jseaes.2018.10.012.

Clark, P.U., Archer, D., Pollard, D., Blum, J.D., Rial, J.A., Brovkin, V., Mix, A.C., Pisias, N.G., Roy, M., 2006. The middle Pleistocene transition: characteristics, mechanisms, and implications for long-term changes in atmospheric pCO_2. Quat. Sci. Rev. 25, 3150–3184. https://doi.org/10.1016/j.quascirev.2006.07.008.

Clemens, S.C., Kuhnt, W., LeVay, L.J., The Expedition 353 Scientists, 2016. Proceedings of the International Ocean Discovery Program. Vol. 353https://doi.org/10.14379/iodp.proc.353.105.2016.

Clift, P.D., Kulhanek, D.K., Zhou, P., Bowen, M.G., Vincent, S.M., Lyle, M., Hahn, A., 2019. Chemical weathering and erosion responses to changing monsoon climate in the late Miocene of Southwest Asia. Geol. Mag. 1–17. https://doi.org/10.1017/S0016756819000608.

Curray, J.R., Emmel, F.J., Moore, D.G., 2002. The Bengal Fan: morphology, geometry, stratigraphy, history and processes. Mar. Pet. Geol. 19, 1191–1223. https://doi.org/10.1016/S0264-8172(03)00035-7.

DeMaster, D.J., 1981. The supply and accumulation of silica in the marine environment. Geochim. Cosmochim. Acta 45, 1715–1732. https://doi.org/10.1016/0016-7037(81)90006-5.

DeMenocal, P.B., 1995. Plio-Pleistocene African climate. Science 270, 53–59. https://doi.org/10.1126/science.270.5233.53.

France-Lanord, C., Derry, L., Michard, A., 1993. Evolution of the Himalaya since Miocene time: isotopic and sedimentological evidence from the Bengal Fan. Geol. Soc. Lond., Spec. Publ. 74, 603–621. https://doi.org/10.1144/GSL.SP.1993.074.01.40.

Gebregiorgis, D., Hathorne, E.C., Giosan, L., Clemens, S., Nürnberg, D., Frank, M., 2018. Southern Hemisphere forcing of south Asian monsoon precipitation over past ~1 million years. Nat. Commun. 9, 4702. (2018). https://doi.org/10.1038/s41467-018-07076-2.

George, M.D., Kumar, M.D., Naqvi, S.W.A., Banerjee, S., Narvekar, P.V., De Sousa, S.N., Jayakumar, D.A., 1994. A study of the carbon dioxide system in the northern Indian Ocean during premonsoon. Mar. Chem. 47, 243–254. https://doi.org/10.1016/0304-4203(94)90023-X.

Govil, P., Naidu, P.D., 2011. Variations of Indian monsoon precipitation during the last 32 kyr reflected in the surface hydrography of the Western Bay of Bengal. Quat. Sci. Rev. 30, 3871–3879. https://doi.org/10.1016/j.quascirev.2011.10.004.

Gupta, A.K., Singh, R.K., Joseph, S., Thomas, E., 2004. Indian Ocean high-productivity event (10–8 Ma): Linked to global cooling or to the initiation of the Indian monsoons? Geology 32, 753–756. https://doi.org/10.1130/G20662.1.

Herbert, T.D., Peterson, L.C., Lawrence, K.T., Liu, Z., 2010. Tropical Ocean temperatures over the past 3.5 million years. Science 328, 1530–1534. https://doi.org/10.1126/science.1185435.

Huang, Y., Clemens, S.C., Liu, W., Wang, Y., Prell, W.L., 2007. Large-scale hydrological change drove the late Miocene C4 plant expansion in the Himalayan foreland and Arabian Peninsula. Geology 35, 531–534. https://doi.org/10.1130/G23666A.1.

Johnson, J.E., Phillips, S.C., Torres, M.E., Piñero, E., Rose, K.K., Giosan, L., 2014. Influence of total organic carbon deposition on the inventory of gas hydrate in the Indian continental margins. Mar. Pet. Geol. 58, 406–424. https://doi.org/10.1016/j.marpetgeo.2014.08.021.

Lee, J., Kim, S., Lee, J.I., Cho, H.G., Phillips, S.C., Khim, B.-K., 2020. Monsoon-influenced variation of clay mineral compositions and detrital Nd-Sr isotopes in the western Andaman Sea (IODP Site U1447) since the late Miocene. Palaeogeogr. Palaeoclimatol. Palaeoecol. 538, 109339. https://doi.org/10.1016/j.palaeo.2019.109339.

Li, J., Fang, X., Song, C., Pan, B., Ma, Y., Yan, M., 2014. Late Miocene–Quaternary rapid stepwise uplift of the NE Tibetan Plateau and its effects on climatic and environmental changes. Quat. Res. 81, 400–423. https://doi.org/10.1016/j.yqres.2014.01.002.

Li, P., Zhang, C., Guo, Z., Deng, C., Ji, X., Jablonski, N.G., Wu, H., Zhu, R., 2019. Clay mineral assemblages in the Zhaotong Basin of southwestern China: implications for the late Miocene and Pliocene evolution of the South Asian monsoon. Palaeogeogr. Palaeoclimatol. Palaeoecol. 516, 90–100. https://doi.org/10.1016/j.palaeo.2018.11.039.

Lisiecki, L.E., Raymo, M.E., 2005. A Pliocene-Pleistocene stack of 57 globally distributed benthic $\delta^{18}O$ records. Paleoceanography 20, PA1003. https://doi.org/10.1029/2004PA001071.

Lu, H., Wang, X., Li, L., 2010. Aeolian sediment evidence that global cooling has driven late Cenozoic stepwise aridification in Central Asia. Geol. Soc. Lond. Spec. Publ. 342, 29–44. https://doi.org/10.1144/SP342.4.

Madhupratap, M., Gauns, M., Ramaiah, N., Kumar, S.P., Muraleedharan, P., De Sousa, S., Sardessai, S., Muraleedharan, U., 2003. Biogeochemistry of the Bay of Bengal: physical, chemical and primary productivity characteristics of the central and western Bay of Bengal during summer monsoon 2001. Deep Sea Res. Part II 50, 881–896. https://doi.org/10.1016/S0967-0645(02)00611-2.

Maslin, M.A., Li, X.S., Loutre, M.F., Berger, A., 1998. The contribution of orbital forcing to the progressive intensification of northern hemisphere glaciation. Quat. Sci. Rev. 17, 411–426. https://doi.org/10.1016/S0277-3791(97)00047-4.

Meyers, P.A., 1994. Preservation of elemental and isotopic source identification of sedimentary organic matter. Chem. Geol. 114, 289–302. https://doi.org/10.1016/0009-2541(94)90059-0.

Miller, K.G., Kominz, M.A., Browning, J.V., Wright, J.D., Mountain, G.S., Katz, M.E., Sugarman, P.J., Cramer, B.S., Christie-Blick, N., Pekar, S.F., 2005. The Phanerozoic record of global sea-level change. Science 310, 1293–1298. https://doi.org/10.1126/science.1116412.

Miranda, J., Baliarsingh, S., Lotliker, A., Sahoo, S., Sahu, K., Kumar, T., 2019. Long-term trend and environmental determinants of phytoplankton biomass in coastal waters of northwestern Bay of Bengal. Environ. Monit. Assess. 192, 55. https://doi.org/10.1007/s10661-019-8033-8.

Mohan, K., Gupta, A.K., 2011. Intense deep convective mixing in the southeast Arabian Sea linked to strengthening of the northeast Indian monsoon during the middle Pliocene (3.4 Ma). Curr. Sci. 101, 543.

Mohtadi, M., Prange, M., Steinke, S., 2016. Palaeoclimatic insights into forcing and respons of monsoon rainfall. Nature 533, 191–199. https://doi.org/10.1038/nature17450.

Mortlock, R.A., Froelich, P.N., 1989. A simple method for the rapid determination of biogenic opal in pelagic marine sediments. Deep Sea Res. Part A 36, 1415–1426. https://doi.org/10.1016/0198-0149(89)90092-7.

Naidu, P.D., Malmgren, B.A., 1999. Quaternary carbonate record from the equatorial Indian Ocean and its relationshi with productivity changes. Mar. Geol. 161, 49–62. https://doi.org/10.1016/S0025-3227(99)00055-9.

Narvekar, J., Kumar, S.P., 2014. Mixed layer variability and chlorophyll *a* biomass in the Bay of Bengal. Biogeosciences 11, 3819–3843. https://doi.org/10.5194/bg-11-3819-2014.

Nelson, D.M., Tréguer, P., Brzezinski, M.A., Leynaerts, A., Quéguiner, B., 1995. Production and dissolution of biogenic silica in the ocean: revised global estimates, comparison with regional data, and relationship to biogenic sedimentation. Glob. Biogeochem. Cycles 9, 359–372. https://doi.org/10.1029/95GB01070.

Officer, C., Ryther, J., 1980. The possible importance of silicon in marine eutrophication. Mar. Ecol. 3, 83–91. https://doi.org/10.1023/A:1021392618824.

Ota, Y., Kawahata, H., Kuroda, J., Yamaguchi, A., Suzuki, A., Araoka, D., Abe-Ouchi, A., Yamada, Y., Ijiri, A., Kanamatsu, T., 2018. Indian monsoonal variations during the past 80 kyr recorded in NGHP-02 Hole 19B, western Bay of Bengal: implications from chemical and mineral properties. Geochem. Geophys. Geosyst. 20, 148–165. https://doi.org/10.1029/2018GC007772.

Ota, Y., Kuroda, J., Yamaguchi, A., Suzuki, A., Araoka, D., Ishimura, T., Kawahata, H., 2019. Monsoon-influenced variations in plankton community structure and upper-water column stratification in the western Bay of Bengal during the past 80 ky. Palaeogeogr. Palaeoclimatol. Palaeoecol. 521, 138–150. https://doi.org/10.1016/j.palaeo.2019.02.020.

Paul, J.T., Ramaiah, N., Sardessai, S., 2008. Nutrient regimes and their effect on distribution of phytoplankton in the Bay of Bengal. Mar. Environ. Res. 66, 337–344. https://doi.org/10.1016/j.marenvres.2008.05.007.

Phillips, S.C., Johnson, J.E., Giosan, L., Rose, K., 2014. Monsoon-influenced variation in productivity and lithogenic sediment flux since 110 ka in the offshore Mahanadi

Basin, northern Bay of Bengal. Mar. Pet. Geol. 58, 502–525. https://doi.org/10.1016/j.marpetgeo.2014.05.007.
Prasanna Kumar, S., Muraleedharan, P., Prasad, T., Gauns, M., Ramaiah, N., De Souza, S., Sardesai, S., Madhupratap, M., 2002. Why is the Bay of Bengal less productive during summer monsoon compared to the Arabian Sea? Geophys. Res. Lett. 29, 2235. https://doi.org/10.1029/2002GL016013.
Prasanna Kumar, S., Nuncio, M., Narvekar, J., Kumar, A., Sardesai, D.S., De Souza, S., Gauns, M., Ramaiah, N., Madhupratap, M., 2004. Are eddies nature's trigger to enhance biological productivity in the Bay of Bengal? Geophys. Res. Lett. 31, 7. https://doi.org/10.1029/2003GL019274.
Prasanna Kumar, S., Nuncio, M., Ramaiah, N., Sardesai, S., Narvekar, J., Fernandes, V., Paul, J.T., 2007. Eddy-mediated biological productivity in the Bay of Bengal during fall and spring intermonsoons. Deep Sea Res. Part I 54, 1619–1640. https://doi.org/10.1016/j.dsr.2007.06.002.
Ragueneau, O., Tréguer, P., Leynaert, A., Anderson, R.F., Brzezinski, M.A., DeMaster, D.J., Dugdale, R.C., Dymond, J., Fischer, G., François, R., Heinze, C., Maier-Reimer, E., Martin-Jézéquel, V., Nelson, D.M., Quéguiner, B., 2000. A review of the Si cycle in the modern ocean: recent progress and missing gaps in the application of biogenic opal as a paleoproductivity proxy. Glob. Planet. Chang. 26, 317–365. https://doi.org/10.1016/S0921-8181(00)00052-7.
Ramaswamy, V., Gaye, B., 2006. Regional variations in the fluxes of foraminifera carbonate, coccolithophorid carbonate and biogenic opal in the northern Indian Ocean. Deep Sea Res. Part I 53, 271–293. https://doi.org/10.1016/j.dsr.2005.11.003.
Reichart, G.J., Lourens, L.J., Zachariasse, W.J., 1998. Temporal variability in the northern Arabian Sea Oxygen Minimum Zone (OMZ) during the last 225,000 years. Paleoceanogr. Paleocl. 13, 607–621. https://doi.org/10.1029/98PA02203.
Rohling, E., Foster, G.L., Grant, K., Marino, G., Roberts, A., Tamisiea, M.E., Williams, F., 2014. Sea-level and deep-sea-temperature variability over the past 5.3 million years. Nature 508, 477–482. https://doi.org/10.1038/nature13230.
Sabine, C.L., Key, R.M., Feely, R.A., Greeley, D., 2002. Inorganic carbon in the Indian Ocean: distribution and dissolution processes. Glob. Biogeochem. Cycles 16, 1067. https://doi.org/10.1029/2002GB001869.
Sarma, V., Rao, G., Viswanadham, R., Sherin, C., Salisbury, J., Omand, M.M., Mahadevan, A., Murty, V., Shroyer, E.L., Baumgartner, M.J.O., 2016. Effects of freshwater stratification on nutrients, dissolved oxygen, and phytoplankton in the Bay of Bengal. Oceanogr. Mar. Biol. Annu. Rev. 29, 222–231. https://doi.org/10.5670/oceanog.2016.54.
Schott, F.A., McCreary Jr., J.P., 2001. The monsoon circulation of the Indian Ocean. Prog. Oceanogr. 51, 1–123. https://doi.org/10.1016/S0079-6611(01)00083-0.
Sijinkumar, A.V., Nath, B.N., Guptha, M.V.S., 2010. Late Quaternary record of pteropod preservation from the Andaman Sea. Mar. Geol. 275, 221–229. https://doi.org/10.1016/j.margeo.2010.06.003.
Smith, H.E.K., Poulton, A.J., Garley, R., Hopkins, J., Lubelczyk, L.C., Drapeau, D.T., Rauschenberg, S., Twining, B.S., Bates, N.R., Balch, W.M., 2017. The influence of environmental variability on the biogeography of coccolithophores and diatoms in the Great Calcite Belt. Biogeosciences 14, 4905–4925. https://doi.org/10.5194/bg-14-4905-2017.
Stein, R., 1991. Accumulation of Organic Carbon in Marine Sediments. Springer-Verlage, Berlin. https://doi.org/10.1007/BFb0010382. (217 pp).
Tang, H., Micheels, A., Eronen, J.T., Ahrens, B., Fortelius, M., 2013. Asynchronous responses of East Asian and Indian summer monsoons to mountain uplift shown by regional climate modelling experiments. Clim. Dyn. 40, 1531–1549. https://doi.org/10.1007/s00382-012-1603-x.
Unger, D., Ittekkot, V., Schäfer, P., Tiemann, J., Reschke, S., 2003. Seasonality and interannual variability of particle fluxes to the deep Bay of Bengal: influence of riverine input and oceanographic processes. Deep Sea Res. Part II 50, 897–923. https://doi.org/10.1016/S0967-0645(02)00612-4.
Wang, P., Clemens, S.C., Tada, R., Murray, R.W., 2019. Blowing in the monsoon wind. Oceanogrpahy 32 (1), 48–59. https://doi.org/10.5670/oceanog.2019.119.
Webster, P., Fasullo, J., 2003. Encyclopedia of Atmospheric Sciences. Academic, New York, pp. 1370–1385.
Webster, P.J., Magana, V.O., Palmer, T., Shukla, J., Tomas, R., Yanai, M., Yasunari, T., 1998. Monsoons: Processes, predictability, and the prospects for prediction. J. Geophys. Res. Oceans 103, 14451–14510. https://doi.org/10.1029/97JC02719.
Zhang, R., Jiang, D., Liu, X., Tian, Z., 2012. Modeling the climate effects of different subregional uplifts within the Himalaya-Tibetan Plateau on Asian summer monsoon evolution. Chin. Sci. Bull. 57, 4617–4626. https://doi.org/10.1007/s11434-012-5284-y.